Observations of ozone production in a dissipating tropical convective cell during TC4

Gary A. Morris[1], Anne M. Thompson[2], Eric J. Bucsela[3], Paul A. Kucera[4], Kenneth E. Pickering[5], Brett F. Taubman[6], Alex M. Bryan[7,8], David Lutz[1], John E. Yorks[9], Danielle Slotke[7], and Kelsey Obenour[7]

[1]Dept. of Physics and Astronomy, Valparaiso University, Valparaiso, IN
[2]Dept. of Meteorology, Pennsylvania State University, University Park, PA
[3]SRI International, Menlo Park, CA
[4]Research Applications Laboratory, NCAR, Boulder, CO
[5]Atmospheric Chemistry and Dynamics Branch, Laboratory for Atmospheres, NASA Goddard Space Flight Center, Greenbelt, MD
[6]Dept. of Chemistry, Appalachian State University, Boone, NC
[7]Dept. of Geography and Meteorology, Valparaiso University, Valparaiso, IN
[8]Dept. of Atmospheric, Oceanic, and Space Sciences, University of Michigan, Ann Arbor, MI
[9]Mesoscale Atmospheric Processes Branch, NASA Goddard Space Flight Center, Greenbelt, MD

Abstract. From 13 July – 9 August 2007, the Nittany Atmospheric Trailer and Integrated Validation Experiment (NATIVE) team launched 25 ozonesondes as part of the Tropical Composition, Cloud, and Climate Coupling (TC4) mission. On 5 August 2007, a strong convective cell formed in the Gulf of Panama. World Wide Lightning Location Network (WWLLN) data indicated 563 flashes between 0900 and 1700 UTC in and around the Gulf. NO_2 data from the Ozone Mapping Instrument (OMI) show enhancements near Panama, suggesting lightning production of NO_x. At 1505 UTC an ozonesonde ascended into the southern edge of the now dissipating convective cell as it moved ashore and west across the Azuero Peninsula. Due to condensation and/or down drafts, the balloon ascended from 2.5 to 5.1 km five times between 1512 and 1700, providing a unique examination of ozone photochemistry on the edge of a convective cell. Ozone at these altitudes increased 4 – 12 ppb between the first and last ascent, resulting cell wide in ~3.3×10^6 moles of ozone (assuming uniform production), of which only ~30% can be explained by descent. This estimate agrees reasonably well with our estimates of lightning ozone production from the WWLLN (~2.2×10^6 moles), from the radar inferred lightning flash data (~1.9×10^6 moles), and from the OMI NO_2 data (~2.6×10^6 moles), though all estimates have large uncertainties.

1. Introduction

The role of lightning in global ozone (O_3) formation has been studied extensively in the latter half of the 20th Century [e.g., *Kroening & Ney*, 1962; *Orville*, 1967; *Griffing*, 1977; *Levine, et al.*, 1981] when it was realized that lightning is a significant contributor to the Earth's reactive nitrogen (NO_x) budget [*Noxon*, 1976; *Peyrous & Lepeyre*, 1982; *Franzblau and Popp*, 1989]. With refinements in regional and global models and lightning flash data from satellites and ground-based networks, the global lightning NO_x (LNO_x) budget has been reliably set at 2 – 8 Tg N/year [*Pickering et al.*, 2009; *Schuman and Huntrieser*, 2007]. *Grewe* [2007] estimates the global lightning contribution to tropospheric O_3 at > 30% with the fractional source greatest in the tropics.

Martin et al. [2007] used SCIAMACHY data to show enhancements of 10 – 15 Dobson units (DU) of O_3 and $(2 – 6) \times 10^{14}$ molecules/cm^2 of NO_2 over the tropical Atlantic and Africa resulting from lightning, with the largest enhancements observed downwind of convection. Ozonesonde data taken in the summer of 2006 aboard the Ron Brown off the Atlantic coast of Africa show a 7 DU increase in tropospheric column O_3 during June as a result of biomass burning in Central Africa and lightning over west Africa [*Jenkins, et al.*, 2008].

Several sources of O_3 data near convective systems have produced a wide range of results. *Schlanta and Moore* [1972] examined sonde data and found high O_3 aloft (2 – 3 times pre-storm ground level concentrations) associated with thunderstorms. *Clark and Griffing* [1985] observed large spikes in O_3 (> 500 ppb in a background of ~200 ppbv) on their research aircraft downwind of a thunderstorm near Baltimore, MD in August 1980. *Dickerson et al.* [1987] show PRE-STORM project (1985) data with the highest O_3 concentrations near 5 km (see their Table 1) and a local max at 10 km near the anvil of a thunderstorm. *Minschwaner et al.* [2008] present evidence that coronal discharges associated with convective cells produce ~20% of the total O_3 from a storm (with the remainder from photochemical production due to LNO_x), while *Jadhav et al.* [1996] suggest direct lightning production of ozone is limited to < 2 – 3% of the total.

Salzmann et al. [2008], on the other hand, used data from TOGA COARE/CEPEX to model the photochemistry in regions of deep convection and found O_3 losses, with a maximum loss at ~5 km (see their Figure 10). Aircraft data from the NOAA P3-B taken during the NASA Pacific Exploratory Mission – Tropics B found no evidence for O_3 or CO production by lightning, but found 1.2×10^{22} molecules/m/flash of NO and O_3 decreases of 6 – 8 ppb (26 – 28 ppb in clear air to ~20 ppb in the convective system) [*Ridley et al.*, 2006]. *Ott et al.* [2007] report modeled losses of O_3 for the 21 July 1998 European Lightning Nitrogen Oxides Project storm, with maximum losses of 9 ppb at 5.5 km during the 3 hours of the storm. Downstream of the storm, they found O_3 production of 1.5 ppb/day, with a maximum change of 5 ppb/day at 5.5 km, while *DeCaria et al.* [2005] found a maximum increase in O_3 production at 9 km of 10 ppb/day. For a tropical case sampled by sondes and the DC-8 over Brazil in 1992, air in the 8 – 12 km convective outflow layer enriched by 1 ppbv NO from lightning produced 7 – 8 ppbv/day of O_3 [*Pickering et al.*, 1996; *Thompson et al.*, 1997].

Laboratory studies have suggested that direct production of O_3 occurs mainly during the pre-discharge period of storms [*Peyrous & Lapeyre*, 1982], and *Franzblau* [1991] found (1) little O_3 production except at very low energies, (2) large decreases in O_3 immediately after discharges, and (3) nearly full recovery to pre-discharge levels after ~10 min. (see his Figure 1).

Several recent studies have used strategically-designed ozonesonde networks [*Thompson,* 2009] to evaluate lightning contributions to the tropospheric O_3 budget. Sonde profiles provide a consistent framework for observing impacts of lightning from the surface to lower stratosphere and for relating O_3 variability to meteorological changes day-to-day. During INTEX-A (Inter-continental Transport Experiment [*Singh et al.*, 2006]) analyses of ~300 profiles collected July-August 2004 over North America (the IONS-04 [INTEX Ozonesonde Network Study] series [*Thompson et al.*, 2007a]) provided several insights. By combining FLEX-PART trajectories [*Stohl et al.*, 1998, 2005] and lightning flash maps with the sonde data filtered to eliminate stratospheric air masses, *Cooper et al.* [2006] deduced that within the middle to upper tropo-sphere (9 – 12 km), up to 80% of the O_3 above background originated from LNO. *Thompson et al.* [2007b] used O_3 laminae from the IONS-04 soundings with tracers (lightning maps, potential vorticity, and satellite images of CO and absorbing aerosols) to compute a four-term O_3 budget for each tropospheric O_3 profile. From these budgets it was determined that 15 – 20% of the tro-pospheric O_3 column over northeastern North America was associated with lightning or pollution introduced into the free troposphere by convection. A limitation of the *Thompson et al.* [2007b] analysis is that lightning contributions older than about a week are not distinguished from other sources of aged, background O_3. *Pfister et al.* [2008] addressed the issue using tagged NO_x sources in a chemical transport model to conclude that an average of 10 ± 2% of tropospheric O_3 in the IONS-04 series originated from lightning.

The summertime IONS-06 soundings [*Thompson et al.*, 2008] included approximately 300 profiles collected August – September 2006, from Mexico City to Canada and from the west to east coasts of the United States (US), providing further insights into the lightning – O_3 connec-tion. In *Thompson et al.* [2008] laminar-based budgets implicated lightning in upper tropo-spheric (UT) O_3 enhancements over Houston and Mexico City, although stratospheric O_3 from the extra-tropics was the dominant player over Houston in the latter third of the campaign. The dominance of lightning as a UT O_3 source over the south central US emerged from IONS-06 in the FLEX-PART analysis by *Cooper et al.* [2007], as it had in IONS-04.

The more subtropical of the IONS-06 soundings pointed to the complexity of processes affecting O_3 profile structure during the early stages of the North American monsoon period, when near-daily convection is ascendant over places like Mexico City. Convective activity excites vertically propagating waves that are detected in laminar analysis [*Grant et al.*, 1998; *Loucks*, 2007; *Thompson et al.*, 2007a,b; 2008]. The TC4 campaign [*Toon et al.*, 2009, this issue] was an excellent vehicle to further investigate wave activity, lightning, and O_3 responses in a highly convective environment, closer to the Intertropical Convergence Zone than the August – September IONS-06 soundings. The concentration of new satellite products and aircraft instrumentation focused on convection were intended to quantify lightning, to relate flashes to improved representations in models, and to link the latter to validation of NO_2 from the Ozone Measuring Instrument (OMI) aboard the NASA Aura satellite, for example [*Bucsela et al.*, 2009, this issue].

In addition to O_3 measurements on the three TC4 aircraft, O_3 profiles were provided through soundings at the Southern Hemisphere Additional OZonedondes (SHADOZ) [*Thompson et al.*, 2003] Costa Rican station (Heredia, 10^0N, 84^0W) and at the TC4 ground site at Las Tablas, Panama (7.75^0N, 80.25^0W; see also *Thompson et al.* [2009, this issue]). Free tropospheric (FT) and lower stratospheric wave signatures were identified in virtually all the Costa Rican and Panama soundings, with an incidence in the tropical tropopause layer (TTL) of > 40% (see Figure 2a in *Thompson et al.* [2009, this issue]). Case studies of O_3 within segments affected by gravity waves demonstrated a clear link to convective activity, as viewed through aircraft tracers, cloud lidar and radar, satellite NO_2, and lightning network imagery.

The 25 Panama sondes, in a region with a high convective frequency during TC4 [*Toon et al.*, 2009, this issue], displayed prominent wave activity associated with convection near the beginning of the mission (13 – 22 July 2007) and after 2 August 2007, when the TC4 aircraft coordinated sampling south of Costa Rica, in the vicinity of the Panama Bight, and as far south as the Galapagos. During the second convective period on 5 August, a day when all three TC4 aircraft flew over the Panama Bight, the ozonesonde launched from Las Tablas was caught in a convective system that kept it oscillating between 2.5 and 5.1 km for nearly two hours before it resumed normal ascent. Though many previous studies have provided profiles before and after convection, this ozonesonde data set is unique in providing insights into changing O_3 concentrations inside a dissipating tropical convective cell. Ozone increased throughout the oscillatory period, and we trace the cause to lightning photochemistry. The following sections provide background with experimental details (Section 2), observations (Section 3), and a summary (Section 4).

2. Background

2.1 NPOL Radar

The NASA polarimetric Doppler weather radar (NPOL) is a S-Band system operating at a frequency of 2.8 GHz (10 cm wavelength). It has horizontal and vertical beam widths of 1.4°. The antenna is a flat passive array instead of the typical parabolic dish. The design allows the system to be transported easily and allows NPOL to operate in conditions with strong winds (e.g., minimum wind loading). One of the main drawbacks of this design is the signal deteriorates when the antenna is wet [*Theisen et al.*, 2009]. Therefore, periods when there is precipitation at the radar site are excluded from the final quality controlled dataset.

For TC4, NPOL was deployed with NATIVE near Las Tablas. NPOL operated almost continuously 16 July – 12 August 2007, with the exception of the period 1800 UTC 19 July – 0200

UTC 21 July. NPOL scanned with a temporal resolution of 10 min and spatial resolution of 200 m. A 12 tilt scanning strategy was used with elevation angles ranging from 0.7° to 23.3°. A volume scan with a maximum range of 150 km was followed by a long-range (to 275 km) surveillance scan. NPOL measured or derived quantities included standard radar parameters: radar reflectivity (DZ), Doppler velocity (VR), and spectral width (SW); and polarimetric parameters: differential reflectivity (ZDR), differential phase (PhiDP), specific differential phase (KDP), and cross correlation (corrHV) between horizontal and vertical polarizations. Nearly 3500 volume scans are available for studying the convective properties in and around Panama.

A variety of events were observed during TC4, ranging from short-lived unorganized convection to long-lived mesoscale convective systems. Often systems developed over the Gulf of Panama in the late evening, but weakened or dissipated before reaching land in the mid-morning hours. As a result of strong diurnal heating, however, a second maximum in convection was often observed over the mountainous regions of Panama during midday. A more detailed discussion of the convection observed during TC4 can be found in *Kucera and Newman* [2009, this issue].

2.2 NATIVE

Continuous surface O_3 measurements at the Las Tablas site were made on the Nittany Atmospheric Trailer and Integrated Validation Experiment **(**NATIVE**)** during the period 17 July – 8 August 2007 with a Thermo Electron Corporation (TECO) Model 49C Ozone Analyzer using the United States Environmental Protection Agency standard measurement technique (EQOA-0880-047). Carbon monoxide (TECO 48C-TL) and SO_2 (TECO 43C-TLE) were measured at the same time, along with the aerosol size distribution (SMPS). After 29 July, NO and NO_y (TECO 42CY) were also measured continuously. All measurements from the TC4 mission can be found on the web at http://ozone.met.psu.edu/NATIVE/TC4.html.

2.3 World Wide Lightning Location Network

In 2007 the World-Wide Lightning Location Network (WWLLN) [*Rodger et al.*, 2006] consisted of approximately 25 sensors detecting lightning flashes at VLF frequencies of 3 – 30 kHz. Flash data (primarily cloud-to-ground or CG flashes) were obtained in near-real-time by NASA GSFC from WWLLN Director, Robert Holzworth, of the University of Washington. *Bucsela et al.* [2009, this issue] estimated the detection efficiency of the WWLLN network of detectors for total flashes (CG + intracloud or IC flashes) in the TC4 region (over open ocean near Costa Rica and Panama) through comparisons of flash rates from the Costa Rica Lightning Detection Network (CRLDN, which uses the same sensors as the United States National Lightning Detection Network, NLDN [*Cummins et al.*, 1998]) and the Lightning Imaging Sensor (LIS) on the Tropical Rainfall Measuring Mission (TRMM) satellite for six storms. The mean detection efficiency was 0.22 +/- 0.08, in reasonable agreement with, though somewhat higher than the estimate of *Roger et al.* [2006]. There is some indication, however, that the detection efficiency is greater over ocean than over land in this part of the world [*Lay et al.*, 2009].

2.4 OMI

OMI has been collecting data since shortly after its launch in July 2004 [*Levelt, et al.*, 2006]. The instrument is a nadir-viewing spectrometer with a CCD array having wavelength and spatial dimensions, the latter comprising 60 pixels across the flight track. The pixel area at nadir is 13 x 24 km^2, although this value increases by approximately an order of magnitude near the edges of the track. Overpass time is ~1345 local time in the tropics, improving the capability of OMI for observing afternoon convective events as compared with GOME and SCIAMACHY (which have morning overpass times).

The retrieval algorithm for NO_2 from OMI has been described by *Bucsela et al.* [2006, 2008], *Celarier et al*. [2008], and *Wenig et al*. [2008]. It employs a spectral fitting procedure to obtain NO_2 slant column densities (SCDs) from the OMI spectra. Vertical column densities (VCDs) are obtained by dividing SCDs by air mass factors (AMFs), which are derived through radiative transfer calculations. The tropospheric component of the vertical column, resulting from sources that include pollution and lightning, is obtained by removing an unpolluted (here simply called “stratospheric”) component, using a wave-2 analysis in narrow latitude bands. Because of the method used to derive it, the stratospheric VCD is contaminated by small amounts of tropospheric NO_2, which we remove in the present study using output from the GMI model [*Duncan et al*., 2007]. The corrected stratospheric VCD differs from the uncorrected value by approximately 5%.

For the 5 August 2007 analysis, OMI NO_2 data are used to estimate the moles of LNO_x in the region near the Gulf of Panama. Details of the procedure are found in *Bucsela et al*. [2009, *this issue*], but we outline the method here. The first step is the calculation of the tropospheric SCD due to LNO_2, which is given by the total SCD minus the sum of the corrected stratospheric SCD and the tropospheric SCD due to sources other than lightning. This non-lightning tropospheric SCD is obtained by running the GMI model with the lightning source turned off. In these calculations, all SCDs and VCDs are related through AMFs derived using radiative transfer calculations and climatological NO_2 profiles. The LNO_2 slant column is converted to a vertical column of LNOx using a modified AMF that accounts for the vertical distribution of LNO_2 and the photolyis ratio of [NO_2]/[NO_x]. The former is obtained from TC4 aircraft data, and the latter from model calculations. This approach is similar to that described by *Beirle et al.* [2009].

2.5 Ozonesondes

Ozone profiles during TC4 at the Las Tablas site were measured using the electrochemical concentration cell (ECC) type [*Komhyr*, 1986; *Komhyr et al.*, 1995] En-Sci 2Z ozonesonde instruments with 0.5% buffered KI cathode solution. The Jülich Ozone Sonde Intercomparison Experiment (JOSIE) found biases < 5%, a precision of 3–5%, and an accuracy of 5–10% up to 30 km for such sondes [*Smit, et al.*, 2007]. With a typical rise rate of ~5 m/s and a measurement time constant of ~25 s, the effective vertical resolution of O_3 features is ~125 m [see also *Smit et al.*, 2007]. Most launches occurred from 12 – 3 pm local time (1700 – 2000 UTC) to coincide with the ~1345 local solar time overpass of NASA's Aura satellite [*Schoeberl et al.*, 2006].

Pressure, temperature, and relative humidity (RH) measurements were measured by Vaisala RS80-15N radiosondes on each payload, as described in *Thompson et al.* [2003, 2007a]. Payloads also contained global positioning systems (GPS) that provided latitude, longitude, altitude, wind speed, and wind direction data. Pressure readings are validated through comparisons of pressure altitude with GPS altitude. When pressure offsets are observed, they are usually <2 hPa, meaning that tropospheric O_3 mixing ratios are adjusted <~2% (<~0.2% at the surface). Corrections to pressure errors are made through post-flight processing so that at burst altitude, pressure and GPS altitudes agree to within 200 m. For 7 of the launches during TC4, RH data above 300 – 500 hPa appear unreliable. All the ozonesonde data can be found at http://physics.valpo.edu/ozone/tc4data.html.

Although each ozonesonde is internally calibrated before each flight, Figure 1 shows a comparison of NATIVE surface O_3 readings with pre-launch ozonesonde readings from the 23 good flights during TC4. The mean bias (sonde – NATIVE) was –0.4 ± 1.2 ppbv, with a root mean square difference of 1.05 ± 0.76 ppbv.

As further validation, ozonesonde columns are compared with OMI total column ozone [*Bhartia*, 2007; *McPeters et al.*, 2008] for nearby overpasses (< 50 km from launch site). Ozonesonde profiles are integrated to burst altitude, then augmented with either a constant mixing ratio assumption for the upper stratosphere or the Solar Backscatter Ultra-Violet (SBUV) balloon burst climatology of *McPeters et al.* [1997]. For the former case, the difference is 17.5 ± 3.8 DU, while for the latter, the difference is 16.7 ± 6.2 DU, with the sondes higher (by ~6%) than OMI. These results are not inconsistent with the finding that the Paramaribo SHADOZ station (5.8^0N, 55.2^0W) reports columns ~10% higher than OMI [*Thompson et al.*, 2007c].

3. Observations

3.1 NPOL

NPOL observed a large system off the coast of Panama on 5 August 2007. The system developed during overnight hours in the Gulf of Panama and slowly propagated westward toward the Azuero Peninsula. The precipitating system covered an area that was several hundred kilometers in the north-south direction and on the order of 100 km in the west-east direction, with the convective core having a mean area of 5,300 ± 2,400 km^2 between 0900 – 1700 UTC, as indicated by the radar data. The peak in convection occurred around 1311 UTC. Figure 2 shows the reflectivity (DZ) field near the peak in convection at 1255 - 1305 UTC. Reflectivity values ranged from about 0 dBZ in the lighter precipitation areas to a maximum of about 55 dBZ in the embedded convection.

Estimated vertical velocities are derived from NPOL Doppler velocity field through a technique called volume velocity processing (VVP) [*Boccippio*, 1995]. For the 5 August cell, the derived wind in the lower atmosphere was generally from the east at speeds on the order of 10 m s^{-1}. With each time step during which the winds were calculated, however, moderate directional shear appeared, with directions fluctuating from southeast to northeast (in agreement with the ozonesonde observations, see Section 3.5 below).

This convective system generated a significant number of lightning strikes. Figure 2 indicates the location of flashes between 1255 and 1305 UTC as indicated by the WWLLN (see Section 3.3 below), which are well correlated with areas active convection indicated by the NPOL radar data. Here we use cloud top height data from NPOL to estimate lightning flash rates, as suggested by *Price and Rind* [1997]. The parameterization of *Futyan and DelGenio* [2007] predicts the flash rate F (flashes/min/300 km^2) to be

$$F = 0.208(H_{17dB} - H_{0^0C})^{1.8}$$

where H_{17dB} is the storm averaged height (km) of the 17dB radar return signal and H_{0^oC} is the height of the 0^0C (freezing) level. From the ozonesonde data, we find H_{0^oC} is ~4.5 km. From the radar data, we determine hourly averages of H_{17dB} and the area of the storm. The resulting hourly flash estimates for 5 August are shown in Table 1. During the period from the genesis of the cell to the final ascent of the balloon (0900 – 1700 UTC), this parameterization predicts a total of 2300 ± 300 flashes.

We can use the flash data to estimate lightning production of O_3 (LO_3) from LNO. Estimates of LNO vary widely [*Pickering et al.*, 2009; *Huntrieser et al.*, 2008; *Koike et al*., 2007; *Hudman et al.* 2007; *Drapcho et al.* 1983] from a low of 43 moles/flash [*Skamarock et al.*, 2003] to a high of 1100 moles/flash [*Price et al.*, 1997, *Winterath et al.*, 1999]. *Pierce [1970] and Prentice and Mackerras [1977]* estimate the ratio of intra-cloud (IC) flashes to cloud-to-ground (CG) flashes for ~8^0N to be 6.5 – 8.0. Estimates of the NO production efficiency of IC to CG flashes varies from 0.1 [*Price et al.*, 1997] to 1.4 [*Fehr et al.*, 2004]. *Lin et al.* [1988] estimate 30 moles of O_3 are produced per mole of NO_x, (i.e., an ozone production efficiency, OPE, of 30) while more recent studies have found OPE in the range 4 – 12 [*Shon et al.*, 2008; *Wood et al.*, 2009; *Zaveri et al.*, 2003]. (Note: For our calculations of LO_3, we scale the OPE to account for the limited 2-hour period between the first and final ascent and assume that enough sunlight was available on the edge of the cell to drive the photochemistry).

Using the ranges above, we estimate 1.3×10^4 – 2.7×10^7 moles of O_3 could have been produced by this cell. The wide range of estimates owes to the remaining high uncertainty in all of the quantities that go into the calculation. Recalculating with values that we feel are most representative of the conditions for this cell (tropical, marine, etc.: OPE = 2; moles NO/flash = 430 as suggested by *Bucsela et al.* [2009, this issue]; IC:CG NO production efficiency = 1) , we determine our best estimate of LO_3 to be 1.9×10^6 moles.

If we assume direct production of O_3 from the lightning strikes of 300 – 3000 moles/flash, as in *Minschwaner et al.* [2008], this translates into 4.0×10^5 – 2.0×10^7 moles of LO_3 for the flashes between 0900 – 1700 UTC. If we restrict our calculation to the flashes during two-hour period after launch (see Table1), we find a range of 1.4×10^5 – 7.2×10^6 moles of LO_3, with our best estimate being 9.2×10^5 moles.

3.2 NATIVE – eliminate all but the ozone data

Figure 3 shows hourly mean O_3 data at NATIVE for the 13 July – 9 August period, with the mean over the mission as the black dots and the mean ± one standard deviation as the dashed lines. The time is UTC, with Panama local time 5 hours behind. A diurnal cycle shows a daily minimum around 1230 (near dawn) of around 13 ppb with a daily maximum around 1830 (early afternoon) of ~22 ppb. The hourly mean O_3 data from 5 August are shown by the gray dots. Overnight (0030 – 1230 UTC), O_3 values are on the low end of the typical range, hovering around 10 ppb. As the cell moved ashore and rain fell, O_3 decreased, with a minimum of < 5 ppb around 1430. Ozone recovered to more typical values of 20 – 25 ppb by 1930 as the storm moved inland.

3.3 WWLLN and Estimated Ozone Production

WWLLN reported frequent lightning in association with the convective cell over the Gulf of Panama on 5 August. Table 1 summarizes the number of flashes per hour detected in the box defined by the latitude range 7.25^0 – 8.75^0N and longitude range 78.75^0 – 81.25^0W. Figure 2 shows the good correlation between the locations of the lightning flashes and the areas of active convective as seen by the NPOL radar for 1255 – 1305 UTC. Notably (but not shown here), the CRLDN observed few if any lightning flashes over the Gulf of Panama on this day. Given the spatial distribution of lightning flashes observed by the CRLDN, it appears that the Gulf of Panama fell in a shadow of the network.

Using the WWLLN flash data between 0900 – 1700 UTC, we can estimate the associated total LO_3, as we did for the NPOL data above with one further modification. A range of detection efficiencies have been reported for lightning detection networks, with *Boccippio et al.* [2001] reporting a 0.9 efficiency for the NLDN and *Bucsela et al.* [2009, this issue] estimating 0.22 ± 0.08 for the WWLLN. Accounting for the efficiency of the WWLLN, we find 2560 ± 930 flashes between 0900 – 1700 UTC, in reasonable agreement with the NPOL estimate of 2300 ± 300 flashes.

Combining the factors in Section 3.1 above with the WWLLN flash estimate, we find a range of 1.2×10^4 – 4.5×10^7 moles of LO_3, with our best estimate of 2.2×10^6 moles (using values associated with conditions more likely to be found in the present case, as we did for the NPOL calculation above), consistent with the NPOL estimate.

If we assume direct production of O_3 from the lightning strikes of 300 – 3000 moles/flash, as in *Minschwaner et al.* [2008], this translates into $4.7 \times 10^5 - 1.9 \times 10^7$ moles of LO_3 for the flashes between 0900 – 1700 UTC. Unlike the NPOL data, the WWLLN suggests little to no lightning during the period of the sonde oscillation (1500 – 1700 UTC), so this mechanism is not indicated by the WWLLN data for post-launch LO_3.

3.4 OMI NO_2

It is difficult to discern the LNO_2 signal from an examination of Level 2 OMI tropospheric NO_2 and cloud fraction data products that result from the standard retrieval conducted at NASA Goddard Space Flight Center [*Bucsela et al.*, 2006], in part because the Level 2 data have not been cloud screened. With reprocessing that includes removing an estimate of background NO_2 and applying an air mass factor more appropriate for convective outflow [*Bucsela et al.*, 2009, this issue], the LNO_2 becomes more evident. Figure 4 shows a map of the LNO_x field near the Gulf of Panama on 5 August 2007 after reprocessing (considering the NO_x to NO_2 ratio at cloud-outflow levels). The boxed area (~54,000 km^2) contains 1520 +/- 1300 kmol LNO_x, which would result in $(1.5 - 11.4) \times 10^6$ moles of O_3 (depending on the OPE selected). If we scale this estimate to the size of the core of the convective cell observed on the NPOL radar (average area of ~5,300 km^2 from 0900 – 1700 UTC), the estimated LO_3 becomes $(0.15 - 1.1) \times 10^6$ moles of O_3, with a best estimate of $(3.0 \pm 2.6) \times 10^5$ moles, whereas if we scale it to match the area of flashes detected by the WWLLN (~46,000 km^2), we find a range of $(1.3 - 9.7) \times 10^6$ moles of O_3 with a best estimate of $(2.6 \pm 2.2) \times 10^6$ moles. While the uncertainties are large, the values appear to be above background. Furthermore, scaling by the larger area of the WWLLN estimate results in the best agreement with the NPOL and WWLLN LO_3 estimates detailed above.

3.5 Ozonesonde Profiles

The ozonesonde launch on 5 August occurred at 1505 UTC to coincide with the scheduled arrival of the NASA aircraft in the Panama area. At the time of launch, rain was falling as part of the convective cell that had just moved ashore from the east, although no lightning was visible. The surface temperature was ~24^0C with RH of 96% and a surface pressure of ~1003 hPa.

About 20 minutes into the flight, the balloon reached 5.1 km and began to descend. About 15 minutes after that, it began to ascend again. Between launch and ~1700 UTC, the balloon oscillated up and down through the air mass between ~2.5 and ~5.1 km five times, as shown in Figure 5. (Note: Each ascent is color coded so that subsequent figures can be analyzed more easily.) Although the detailed explanation for this behavior is beyond the scope of this paper (see *Morris et al.*, to be submitted to the *American Journal of Physics*, 2009), it appears to be a combination of downdrafts on the southern side of the westward moving convective cell (based on NPOL radar data) and increased mass due to repeated condensation/evaporation of water and freezing/melting of ice on the surface of the balloon.

Figure 6 shows the O_3 concentrations measured on each ascent. Over the ~2 hours between the original ascent and the final ascent, O_3 in the layer between ~2.5 and ~5.1 km increased 4 – 12 ppbv, with a mean increase of 7.9 ± 4.7 ppb. Integrating the change in O_3 between the first and last profiles from 2.55 – 5.11 km (the range of the oscillation), and assuming uniform production in the volume of the storm (5,300 ± 2,400 km^2 as indicated by the NPOL data from 0900 – 1700 UTC, assuming a 2 km depth), we find a potential of ~3.3×10^6 moles of O_3 (with ~50% uncertainty) created as part of this cell, a number that agrees reasonably well with the best estimates from the lightning data (see Sections 3.1 and 3.3) and the OMI data (see Section 3.4 above). We note that the estimates from the lightning data and from OMI represent the total LO_3 throughout the cloud, whereas our sonde only observed the enhancements in the 2.5 – 5.1 km layer. The NPOL radar data, however, indicate that the average height of the 17 dB echo (used as a proxy for cloud height in this study) for the period 0900 – 1700 UTC was 5.24 ± 0.73 km, suggesting that the estimates are indeed comparable.

The total change in O_3 as observed by the balloon is given by

$$\frac{d[O_3]}{dt} = \frac{\partial[O_3]}{\partial t} + \vec{v} \cdot \vec{\nabla}[O_3]$$

where the first term represents in situ photochemical production (loss) and the second term represents changes due to advection. If the balloon had remained at a fixed altitude within the cloud or if the winds were constant with altitude over the vertical range of oscillation, we would assume that the observations were Lagrangian, meaning the advection term would vanish. Figure 7 shows the wind speeds and directions on each ascent of the balloon as determined from on board GPS data. Because of the vertical wind shear within the cell (seen by NPOL and in the balloon data), the advection term may be non-negligible, so we investigate further below.

Table 2 shows the calculated differences between the balloon positions recorded by the GPS and the estimated subsequent positions of the air masses sampled on the first ascent at three levels (2.75, 3.75, and 4.75 ± 0.15 km). To calculate these estimates, trajectories were based upon GPS wind speed and direction data vertically averaged in each of the three layers on successive ascents. The resulting *u* (east-west wind) and *v* (north-south wind) values were multiplied by the time difference between successive ascents to get longitude and latitude displacements. Since the balloon did not oscillate through all three layers each time, the table contains some “No data” entries. These calculations suggest separations of 15 – 30 km between the originally and finally sampled air masses, providing a constraint on the horizontal scale of potential O_3 gradients.

Figure 8 shows the change in O_3 with time as a function of altitude, calculated as the difference between the O_3 at a given altitude as measured on each ascent with that measured on the first ascent. Changes of 3 – 10 ppbv/hr are observed, with the highest rates at 2.5 – 3.0 km between the first and second ascents, and at 3.5 – 4.5 km between the first and third ascents. We note from Table 2 that for the former case, the balloon is located about 5 km upwind from the original air mass, somewhat farther from the center of the storm as it comes ashore. For the latter case, the balloon is located about 13 km downwind of the original air mass, closer to the center of the cell. Since both profiles suggest somewhat large O_3 changes with time, with one being upwind and the other being downwind of the original air masses, it is possible that the advection term over these spatial scales is relatively small.

One last component of the advection term to investigate is the vertical term. While some of the change in O_3 with time is due to descent, most appears due to other factors. First, the original ascending profile in Figure 6 (purple) can be joined with near perfect continuity to the final ascending profile between 5 and 5.5 km, suggesting the O_3 enhancements are not due to air descending from above 5.5 km. Second, Figure 9 shows the change in potential temperature (theta) between the first and final ascent as a function of altitude between 2.55 – 5.11 km. Between 2.55 and ~3.40 km, 1.25 – 2.25 K of warming is observed. Between 3.4 – 5.11 km, 0.25 – 1.0 K of warming is observed. If we assume that the change in theta in the lower layer is due solely to descent, the air found in the 2.55 – 3.40 km layer on the last pass was originally between 3.09 – 3.55 km. The mean O_3 in this layer (defined by theta) on the first pass was 32.1 ± 1.3 ppb while on the last pass, it was 37.9 ± 2.2 ppb, a difference of 5.8 ± 2.6 ppb. If we assume no descent at all, the mean O_3 in this layer (defined by altitude) was 29.5 ± 1.9 ppbv on the first pass, a difference of 8.4 ± 2.9 ppbv. Thus, we attribute 2.6 ± 3.9 ppbv (~31%) of the change to descent of air between the first and last ascents, with air descending at an average rate of 6.2 cm/s. *Zahn et al.* [2002] also found that downdrafts were insufficient to explain enhancements in O_3 and NO_x resulting from thunderstorms as seen by the NOAA WP-3D during the Southern Oxidant Study in 1996.

Finally, Figure 10 shows O_3 as a function of theta rather than height for the first and last ascents. Integrating the change in O_3 as a function of theta between 311.75 – 320.00 K, and assuming the cell size as before, we find an increase of 2.5×10^6 moles of O_3, in good agreement with the estimates from the lightning data detailed above.

HYSPLIT back trajectories [*Draxler and Rolph*, 2003] of air parcels in each of the three layers described in Table 2 (2750, 3750, and 4750 m) were calculated using the Global Data Assimilation System (GDAS) meteorological fields. The course resolution of the GDAS meteorological fields (1^0 latitude $\times$ 1^0 longitude) does not permit detailed analysis of the air mass movement associated with the convective cell, nor do such analyses even approximately capture the vertical motions associated with convection, so such trajectories must always be examined with some caution. Nevertheless, the results indicate that the air masses in these layers of enhancement O_3 remained within the convective cell as it developed over the Gulf of Panama and moved ashore during the previous 6 hours (not shown). Thus, lightning production of NO and the subsequent O_3 photochemistry as the cell dissipated and came ashore appears to be a plausible explanation for the changes observed by the sonde.

4. Summary and Discussion

This work has presented a unique ozonesonde profile over Las Tablas, Panama on 5 August 2007. The balloon was launched on the southern side of a dissipating convective cell as it came ashore from the east. Between 0900 and 1700 UTC, WWLLN data indicate 563 flashes (~2600 flashes accounting for the lightning detection efficiency of this network) in and around the Gulf of Panama, while estimates of lightning flash rates using NPOL radar cloud height data result in ~2300 flashes associated with this cell. The ozonesonde oscillated between ~2.5 and ~5.1 km for ~108 minutes, during which 5 ascents were made through the air mass. Ozone concentrations increased by 4 – 12 ppb over a ~2 hour period between the first and last ascending profile, consistent with the 5 ppb/day suggested near 5 km by *Ott et al.* [2007], the 10 ppb/day near 9 km suggested by *DeCaria et al.* [2005], and the 7 – 8 ppb/day in the 8 – 12 km layer suggested by *Pickering et al.* [1996] and *Thompson et al.* [1997]. The more rapid increase observed by the sonde, however, may suggest that much of the O_3 production occurs soon after daylight returns to the air mass affected by the cell rather than over the course of a day, a hypothesis consistent with the laboratory work of *Franzblau* [1991].

Assuming the changes in O_3 observed by the sonde are representative of the entire cell (~5300 km^2 by 2 km depth), an increase of 3.3×10^6 moles of O_3 may be associated with this storm. Further analysis indicates that descent alone explains only ~30% of the change in O_3 observed. Our ozonesonde LO_3 estimate agrees well with estimates from the WWLLN data (~2.2×10^6 moles), from the NPOL data (~1.9×10^6 moles), and from the OMI LNO_2 data (~2.6×10^6 moles), in the last case provided we scale by the larger area considered with the WWLLN data rather than the convective core area indicated by the NPOL data, and in all cases recognizing the very large associated uncertainties.

Wind profiles from the sonde and NPOL data indicate some vertical divergence within the layer of observed O_3 changes. Subsequent trajectory calculations suggest the possible separation of the originally sampled air mass from that sampled on the final ascent by 15 – 30 km over the ~108 minutes. The changes in O_3 observed by the sonde thus may be attributed to horizontal O_3 gradients with a scale < 30 km and/or in situ photochemistry. In the former case, the original air mass at 2.75 km ends up ~15 km to the southwest of balloon trajectory (see Table 2), so the balloon ends up falling backward relative to the westward moving center of the cell and the original air mass. As O_3 increases, the dynamical explanation would require higher O_3 concentrations outside of the cell in less dense clouds in which photochemical O_3 production may take place and in which loss of O_3 through reactions with NO from lightning may not have occurred. At 3.75 and 4.75 km, however, the trajectories suggest the original air mass ends up 25 – 30 km southeast of the balloon trajectory, resulting in the balloon sampling air closer to the center of the cell. After the last oscillation, the balloon position is on the southeastern edge of the storm, whereas for the first oscillation it was just west of the center of the cell. At these higher altitudes, it would seem that the balloon is sampling air more reflective of the cell core, which suggests O_3 levels within the cell have actually increased.

If lightning and photochemistry are responsible for the changes in O_3, our ozonesonde observations may be consistent with the idea that shortly after the lightning strikes, NO reacts with O_3 forming NO_2 and leading to O_3 loss within the clouds. This hypothesis is supported by the modeling studies of *Ott et al.* [2007] and *Salzmann et al.* [2008], the thunderstorm observations in *Ridley et al.* [2006], and the laboratory data of *Franzblau* [1991]. By the time the convective cell reaches the Panama coast, the lightning has subsided (as suggested by the WWLLN data in Table 1) and the clouds have begun to dissipate. Ozone within the clouds, therefore, may be relatively depleted compared to its pre-storm values, and our balloon measurements may therefore simply represent measurements at various stages of recovery as NO_x photochemistry begins to favor production of O_3.

Alternatively or in addition to the loss/recovery process, new O_3 may have been produced within the cloud, as suggested by *Winterrath et al.* [1999] who report a 62% increase in ozone within the thunderstorm clouds; *Shlanta and Moore* [1972] who found ozone levels 2.6 times higher at 6 km inside the cloud than pre-storm readings at the surface; and *Clark and Griffing* [1985] who reported 250% increases downwind of thunderstorms near Baltimore in 1980. If the dissipating cell was still producing lightning after launch, as suggested by the NPOL hourly flash estimates (Table 2), it is possible that direct production of LO_3 was occurring within the cloud, as suggested by *Minschwaner et al.* [2008].

Given the large uncertainties in all of the LO_3 calculations, the agreement we find in the study is reasonable, although we also note that it is possible that the area of the storm sampled by the ozonesonde contained O_3 changes unrepresentative of the larger cell. In a future modeling study, the unique balloon observations reported here will be combined with DC-8 data to further investigate O_3 production and loss processes associated with deep tropical convection.

Acknowledgments. Funding for this work was provided by NASA's Upper Air Research Program (M.J. Kurylo and K.W. Jucks, program managers). Thanks to the OMI team for the total column ozone data and to Robert Holzworth for the WWLLN lightning data. We also would like to thank the reviewers for their helpful comments for improving our manuscript.

References

Beirle, S., M. Salzmann, M. G. Lawrence, and T. Wagner (2009), Sensitivity of satellite observations for freshly produced lightning NO_x, *Atmos. Chem. Phys.*, *9*, 1077 – 1094.

Bhartia, P.K. (2007), Algorithm Theoretical Basis Document, http://toms.gsfc.nasa.gov/version8/v8toms_atbd.pdf.

Boccippio, D. J. (1995), A diagnostic analysis of the VVP single-Doppler retrieval technique. *J. Atmos. Oceanic Technol.*, *12*, 230-248.

Boccippio, D.J., K.L. Cummins, H.J. Christian, and S.J. Goodman (2001), Combined satellite- and surface-based estimation of intracloud-cloud-to-ground lightning ratio over the continental United States, *Mon. Weath. Rev.*, *129*, 108 – 122.

Boersma, K.F., H.J. Eskes, E.W. Meijer, and H.M. Kelder (2005), Estimates of lightning NOx production from GOME satellite observations, *Atmos. Chem. Phys.*, *5*, 2311 – 2331.

Bucsela E.J., E.A. Celarier, M.O. Wenig, J.F. Gleason, J.P. Veefkind, K.F. Boersma, E.J. Brinksma (2006), Algorithm for NO_2 vertical column retrieval from the Ozone Monitoring Instrument, *IEEE Transactions on Geoscience and Remote Sensing*, *44*, 1245-1258.

Bucsela, E.J., A.E. Perring, R.C. Cohen, K.F. Boersma, E.A. Celarier, J.F. Gleason, M.O. Wenig, T.H. Bertram, P.J. Wooldridge, R. Dirksen, and J.P. Veefkind (2008), Comparison of tropospheric NO_2 from in situ aircraft measurements with near-real-time and standard product data from OMI, *J. Geophys. Res*., *113*, D16S31, doi:10.1029/2007JD008838.

Bucsela, E.J, K.E. Pickering, T. Huntemann, R.C. Cohen, A. E. Perring, J. F. Gleason, R. Blakeslee, D. V. Navano, I. M. Mora Segura, A. P. Hernández, S. Laporte-Molina (2009), Lightning-generated NO_x seen by OMI during NASA's TC^4 experiment, *J. Geophys. Res*., this issue.

Celarier, E. A., E. J. Brinksma, J. F. Gleason, J. P. Veefkind, A. Cede, J. R. Herman, D. Ionov, F. Goutail, J-P. Pommeraeau, J-C. Lambert, M. van Roosendael, G. Pinardi, B. Bojkov, G. Mount, E. Spinei, S. P. Sander, E. J. Bucsela, D. P. J. Swart, H. Volten, M. Kroon, and P. F. Levelt (2008), Validation of Ozone Monitoring Instrument nitrogen dioxide columns, *J. Geophys. Res*., *113*, D15S15, doi:10.1029/2007JD008908.

Clark, J.F., and G.W. Griffing (1985), Aircraft observations of extreme ozone concentrations near thunderstorms, *Atmos. Environ.*, *19*, 7, 1175 – 1179.

Cooper, O. R., et al. (2006), Large upper tropospheric ozone enhancements above mid-latitude North America during summer: In situ evidence from the IONS and MOZAIC ozone networks, *J. Geophys. Res.*, *111*, D24S05, doi: 10.1029/2006JD007306.

Cooper, O.R, et al. (2007), Evidence for a recurring eastern North America upper tropospheric ozone maximum during summer, *J. Geophys. Res.*, *112, D23304*, doi: 10.1029/2007JD008710.

Cummins, K.L., M.J. Murphy, E.A. Bardo, W.L. Hiscox, R.B. Pyle, and A.E. Pifer (1998), A combined TOA/MDF technology upgrade of the U.S. Lightning Detection Network, *J. Geophys. Res.*, *103*, D8, 9035 – 9044.

DeCaria, A.J., K.E. Pickering, G.L. Stenchikov, and L.E. Ott (2005), Lightning-generated NOx and its impact on tropospheric ozone production: A three-dimensional modeling study of a Stratospher-Troposphere Experiment: Radiation, Aerosols and Ozone (STERAO-A) thunderstorm, *J. Geophys. Res.*, *110(D14)*, D14303, doi:10.1029/2004JD005556.

Dickerson, R.R., G.J. Huffman, W.T. Luke, L.J. Nunnermacker, K.E. Pickering, A.C.D. Leslie, C.G. Lindsey, W.G.N. Slinn, T.J. Kelly, P.H. Daum, A.C. Delany, J.P. Greenberg, P.R. Zimmerman, J.F. Boatman, J.D. Ray, and D.H. Stedman (1987), Thunderstorms: An important mechanicsm in the transport of air pollutants, *Science*, *235*, 460 – 465.

Drapcho, D.L., D. Sisterson, and R. Kumar (1983), Nitrogen fixation by lightning activity in a thunderstorm, *Atmos. Environ.*, *17*, 729 – 734.

Draxler, R.R. and Rolph, G.D. (2003), HYSPLIT (HYbrid Single-Particle Lagrangian Integrated Trajectory) Model access via NOAA ARL READY Website (http://www.arl.noaa.gov/ready/hysplit4.html). NOAA Air Resources Laboratory, Silver Spring, MD.

Duncan, B. N., S. E. Strahan, Y. Yoshida, S. D. Steenrod, and N. Livesey (2007), Model study of the cross-tropopause transport of biomass burning pollution, *Atmos. Chem. Phys., 7*, 3713-3736.

Fehr, T., H. Holler, and H. Huntrieser (2004), Model study on production and transport of lightning-produced NOx in a EULINOX supercell storm, *J. Geophys. Res., 109(D9)*, D09102, doi:10.1029/2003JD003935.

Folkins, I., C. Braun, A.M. Thompson, and J. Witte (2002), Tropical ozone as an indicator of deep convection, *J. Geophys. Res., 107*, 4184, 10.1029/2001JD001178.

Franzblau, E., and C.J. Popp (1989), Nitrogen oxides produced from lightning, *J. Geophys. Res., 94*, 11,089 – 11,104.

Franzblau, E. (1991), Electrical discharges involving the formation of NO, NO2, HNO3, and O3, *J. Geophys. Res., 96*, D12, 22,337 – 22,345.

Futyan, J.M., and A.D. Del Genio (2007), Relationships between lightning and properties of convective cloud clusters. *Geophys. Res. Lett. 34*, L15705, doi:10.1029/2007GL030227.

Grant, W. B., R. B. Pierce, S.J. Oltmans, E.V. Browell (1998), Seasonal evolution of total and gravity wave induced laminae in ozonesonde data in the tropics and subtropics, *Geophys. Res. Lett., 25*, 1863-1866.

Grewe, V. (2007), The impact of climate variability on tropospheric ozone, *Science of the Total Environment, 374*, 167 – 181.

Griffing, G.W. (1977), Ozone and oxides of nitrogen production during thunderstorms, *J. Geophys. Res., 82*, 943 – 950.

Hudman, R.C., et al. (2007), Surface and lightning sources of nitrogen oxides over the United States: Magnitudes, chemical evolution, and outflow, *J. Geophys. Res., 112*, D12S05, doi:10.1029/2006JD007912.

Huntrieser, H., H. Schlager, H. Höller, U. Schumann, H.D. Betz, D. Boccippio, D. Brunner, C. Forster, and A. Stohl (2006), Lightning-produced NOx in tropical, subtropical and midlatitude thunderstorms: New insights from airborne and lightning observations, *Geophys. Res. Abs., 8*, 03286.

Huntrieser, H., U. Schumann, H. Schlagr, H. Holler, A. Giez, H.D. Betz, D. Brunner, C. Forster, O. Pinto, and R. Calheiros (2008), Lightning activity in Brazilian thunderstorms during TROCCINOX: Implications for NOx production, *Atmos. Chem. Phys., 8(4)*, 921 – 953.

Jadhav, D. B., et al. (1996), Observations of NO2 and O3 during thunderstorm activity using visible spectroscopy, *Adv. Atmos. Sci., 13(3)*, 359-374.

Jenkins, G.S., M. Camara, and S.A. Ndiaye (2008), Observational evidence of enhanced middle/upper tropospheric ozone via convective processes over the equatorial tropical Atlantic during the summer of 2006, *Geophys. Res. Lett., 35*, L12806, doi: 10.1029/2008GL033954.

Koike, M., Y. Kondo, K.Kita, N. Takegawa, N. Nishi, T. Kashihara, S. Kawakami, S. Kudoh, D. Blake, T. Shirai, B. Liley, M. Ko, Y. Miyazaki, Z. Kawaski, and T. Ogawa (2007), Measurements of reactive nitrogen produced by tropical thunderstorms during BIBLE-C, *J. Geophys. Res., 112*, D18304, doi: 10.1029/2006JD008193.

Komhyr, W.D. (1986), Operations Handbook: Ozone measurements to 40 km altitude with mode 4A electrochemical concentration cell (ECC) ozonesondes (used with 1680-Mhz radiosondes), *NOAA Technical Memorandum ERLARL-149*.

Komhyr, W.D., R.A. Barnes, G.B. Brothers, J.A. Lathrop, and D.P. Opperman (1995), Electrochemical concentration cell performance evaluation during STOIC, *J. Geophys. Res., 100*, 9231 – 9244.

Kroening, J., and E. Ney (1962), Atmospheric Ozone, *J. Geophys. Res.*, 67(5), 1867-1875.

Kucera, P. A. and A. J. Newman (2009), Convective characteristics observed over Panama and adjacent Gulf of Panama during TC4. *J. Geophysics. Res*., submitted, this issue.

Lay, E. H., C. J. Rodger, R. H. Holzworth, A. R. Jacobson, D. M. Suszcynsky, J. N. Thomas, and J. B. Brundell (2009), World—wide lightning location network: improvements in global detection efficiency and estimated stroke energy, *Fourth Conference on the Meteorological Applications of Lightning Data,* American Meteorological Society, Phoenix, AZ.

Levelt, P. F., E. Hilsenrath, G.W. Leppelmeier. G. B. J. van den Oord, P. K. Bhartia, J. Tamminen, J. F. de Haan and J. P. Veefkind (2006), Science objectives of the Ozone Monitoring Instrument, *IEEE Trans Geo. Rem. Sens., 44(5),* 1199 – 1208.

Levelt, P. F., G. B. J. van den Oord, M.R. Dobber, A. Malkki, H. Visser, J. deVries, P. Stammes, J.O.V. Lundell, and H. Saari (2006), The Ozone Monitoring Instrument, *IEEE Trans Geo. Rem. Sens., 44(5)*, 1093 – 1101.

Levine, J.S., R.S. Rogowski, G.L. Gregory, W.E. Howell, and J. Fishman (1981). Simultaneous measurements of NOx, NO, and O3 production in a laboratory discharge: Atmospheric implications, *Geophys. Res. Lett., 8*, 4, 357 – 360.

Lin, X., M. Trainer, and S. C. Liu (1988), On the nonlinearity of tropospheric ozone production, *J. Geophys. Res., 93*, 15,879–15,888.

Loucks, A. L. (2007), Evaluation of dynamical sources of ozone laminae in the tropical troposphere and tropical tropopause layer, M.S. Thesis, Penn State University.

Martin, R.V., B. Sauvage, I. Folkins, C.E. Sioris, C. Boone, P. Bernath, and J. Ziemke (2007), Space-based constraints on the production of nitric oxide by lightning, *J. Geophys. Res., 112*, D09309, doi: 10.1029/2006JD007831.

McPeters, R. D., G. J. Labow, and B. J. Johnson (1997), A satellite-derived ozone climatology for balloonsonde estimation of total column ozone, *J. Geophys. Res., 102*(D7), 8875 – 8886.

McPeters, R., M. Kroon, G. Labow, E. Brinksma, D. Balis, I. Petropavlovskikh, J.P. Veefkind, P.K. Bhartia, and P.F. Levelt (2008), Validation of the Aura Ozone Monitoring Instrument total column ozone product, *J. Geophys. Res., 113*, D15S14, doi:10.1029/2007JD008802.

Minschwaner, K., L.E. Kalnajs, M.K. Dubey, L.M. Avallone, P.C. Sawaengphokai, H.E. Edens, and W.P. Winn (2008), Observation of enhanced ozone in an electrically active storm over Socorro, NM: Implications for ozone production from corona discharges, *J. Geophys. Res.*, 113, D17208, doi:10.1029/2007JD009500.

Noxon, J.F. (1976), Atmospheric nitrogen fixation by lightning, *Geophys. Res. Lett., 3*, 8, 463 – 465.

Orville, R.E. (1967), Ozone production during thunderstorms, measured by the absorption of ultraviolet radiation from lightning, *J. Geophys. Res., 72*, 14, 3557 – 3561.

Ott, L.E., K.E. Pickering, G.L. Stenchikov, H. Huntrieser, and U. Schumann (2007), Effects of lightning NOx production during the 21 July European Lightning Nitrogen Oxides Project storm studied with a three-dimensional cloud-scale chemical transport model, *J. Geophys. Res., 112*, D05307, doi: 10.1029/2006JD007365.

Peyrous, R., and R.-M. Lapeyre (1982), Gaseous products created by electrical discharges in the atmosphere and condensation nuclei resulting from gaseous phase reactions, *Atmos. Environ., 16*, 5, 959 – 968.

Pfister, G. G., L. K. Emmons, P. G. Hess, J.-F. Lamarque, A. M. Thompson, J. E. Yorks (2008), Analysis of the Summer 2004 Ozone Budget over North America using IONS Observations and MOZART-4 Simulations, *J. Geophys. Res.*, *113***,** D23306, doi:10.1029/2008JD010190.

Pickering, K.E., A. M. Thompson, Y. Wang, W.-K. Tao, D. P. McNamara, V. W. J. H. Kirchhoff, B. G. Heikes, G. W. Sachse, J. D. Bradshaw, G. L. Gregory, and D. R. Blake (1996), Convective transport of biomass burning emissions over Brazil during TRACE-A, *J. Geophys. Res., 101*, 23,993-24,012.

Pickering, K., H. Huntrieser, and U. Schumann (2009), Chapter 26: Lightning and NOx production in global models in *Lightning: Principles, Instruments and Applications*, H.D. Betz et al. (eds.), doi: 10.1007/978-1-4020-9079-0_26.

Pierce, E. T., (1970), Latitudinal variation of lightning parameters, *J. Appl. Meteor., 9***,** 194–195.

Prentice, S. A., and D. Mackerras (1977), The ratio of cloud to cloudground lightning flashes in thunderstorms, *J. Appl. Meteor., 16*, 545–549.

Price, C., J. Penner, and M. Prather (1997), NOx from lightning 1: Global distribution based on lightning physics, *J. Geophys. Res., 102(D5)*, 5929 – 5941.

Price, C., J. Penner, and M. Prather (1997), NOx from lightning 2: Constraints from the global atmospheric electric circuit, *J. Geophys. Res., 102(D5)*, 5943 – 5951.

Ridley, B.A., M.A. Avery, J.V. Plant, S.A. Vay, D.D. Montzka, A.J. Weinheimer, D.J. Knapp, J.E. Dye, and E.C. Richard (2006), Sampling of chemical constituents in electrically active convective systems: Results and cautions, *J. Atmos. Chem.*, *54*, 1 – 20, doi: 10.1007/s10874-005-9007-5.

Rodger, C. J., S.Werner, J. B. Brundell, E. H. Lay, N. R. Thomson, R. H. Holzworth, and R. L. Dowden (2006), Detection efficiency of the VLF World-Wide Lightning Location Network (WWLLN): initial case study, *Ann. Geophys.*, *24*, 3197–3214.

Rolph, G.D. (2003), Real-time Environmental Applications and Display sYstem (READY) Website (http://www.arl.noaa.gov/ready/hysplit4.html). NOAA Air Resources Laboratory, Silver Spring, MD.

Ryu, J.-H., and G.S. Jenkins (2005), Lightning-tropospheric ozone connections: EOF analysis of TCO and lightning data, *Atmos. Env., 39*, 5799 – 5805.

Salzmann, M., M.G. Lawrence, V.T.J. Phillips, and L.J. Donner (2008), Cloud system resolving model study of the roles of deep convection for photo-chemistry in the TOGA COARE/CEPEX region, *Atmos. Chem. Phys., 8*, 2741-2757.

Schlanta, A., and C.B. Moore (1972), Ozone and point discharge measurements in thunderclouds, *J. Geophys. Res., 77*, 24, 4500 -4510.

Schoeberl, M.R., A.R. Douglass, E. Hilsenrath, P.K. Bhartia, R. Beer, J.W. Waters, M.R. Gunson, L. Froidevaux, J.C. Gille, J.J. Barnett, P.E. Levelt, and P. DeCola (2006), Overview of the EOS Aura Mission, *IEEE Trans. Geoscience and Remote Sensing, 44(5)*, 1066 – 1074.

Schumann U., and H. Huntrieser (2007), The global lightning-induced nitrogen oxides source, *Atmos. Chem. Phys., 7*, 3823 – 3907.

Shon, Z.H., S. Madronich, S.K. Song, F.M. Flocke, D.J. Knapp, R.S. Anderson, R.E. Shetter, C.A. Cantrell, S.R. Hall, and X.Tie (2008), Characteristics of the NO-NO2-O3 system in different chemical regimes during the MIRAGE-Mex field campaign, *Atmos. Chem. Phys., 8(23)*, 7153 – 7164.

Singh, H. B., W. H. Brune, J. H. Crawford, D. J. Jacob, P. B. Russell (2006), Overview of the summer 2004 Intercontinental Chemical Transport Experiment - North America (INTEX-NA), *J. Geophys. Res., 111*, D24S01, doi: 10.1029/2006JD007905.

Skamarock, W.C., J.E. Dye, E. Defer, M.C. Barth, J.L. Stith, B.A. Ridley, and K. Baumann, (2003), Observational- and modeling-based budget of lightning produced NOx in a continental thunderstorm, *J. Geophys. Res., 108(D10)*, 4305, doi:10.1029/2002JD002163.

Smit, H.G., W. Straeter, B.J. Johnson, S.J. Oltmans, J. Davis, D.W. Tarasick, B. Hoegger, R. Stubi, F.J. Schmidlin, T. Northam, A.M. Thompson, J.C. Witte, I. Boyd, and F. Posny (2007), Assessment of the performance of ECC-ozonesondes under quasi-flight conditions in the environmental simulation chamber: Insights from the Jülich Ozone Sonde Intercomparison Experiment (JOSIE), *J. Geophys. Res., 112, D19306*, doi:10.1029/2006JD007308.

Stohl, A., M. Hittenberger, and G. Wotawa (1998), Validation of the Lagrangian particle dispersion model FLEXPART against large scale tracer experiment data, *Atmos. Environ., 32*, 4245–4264.

Stohl, A., C. Forster, A. Frank, P. Seibert, and G. Wotowa (2005), Technical note: The Lagrangian particle dispersion model FLEXPART version 6.2, *Atmos. Chem. Phys., 5*, 2461– 2474.

Theisen, C. J., P. A. Kucera, and M. R. Poellot (2009), A Study of Relationships between Tropical Thunderstorm Properties and Corresponding Anvil Cloud Characteristics, *J. Meteor. and Climate* (in press).

Thompson, A.M., J.C. Witte, R.D. Hudson, H. Guo, J.R. Herman, and M. Fujiwara (2001), Tropical tropspheric ozone and biomass burning, *Science, 291(5511)*, 2128 – 2132.

Thompson, A.M., J.C. Witte, R.D. McPeters, S.J. Oltmans, F.J. Schmidlin, J.A. Logan, M.Fujiwara, V.W.J.H. Kirchhoff, F. Posny, G.J.R. Coetzee, B. Hoegger, S. Kawakami, T. Ogawa, B.J. Johnson, H. Vömel and G. Labow (2003), Southern Hemisphere Additional Ozonesondes (SHADOZ) 1998-2000 tropical ozone climatology 1. Comparison with Total Ozone

Mapping Spectrometer (TOMS) and ground-based measurements, *J. Geophys. Res., 108(D2)*, 8238, doi: 10.1029/2001JD000967.

Thompson, A.M., J.B. Stone, J.C. Witte, R.B. Pierce, R.B. Chatfield, S.J. Oltmans, O.R. Cooper, B.F. Taubman, B.J. Johnson, E. Joseph, T.L. Kucsera, J.T. Merrill, G.A. Morris, S. Hersey, M.J. Newchurch, F.J. Schmidlin, D.W. Tarasick, V. Thouret, and J.-P. Cammas (2006), IONS-04 (INTEX Ozonesonde Network Study, 2004): Perspective on summertime UT/LS (upper troposphere/lower stratosphere) ozone over Northeaster North America), submitted, *J. Geophys. Res.* (2006JD007441).

Thompson, A. M. (2009), An Overview of Strategic Ozone Sounding Networks: Insights into Ozone Budgets, UT/LS Processes and Tropical Climate Signatures, *Protecting the Ozone Layer*, C. Zerefos, Ed., Springer, Chapter 17.

Thompson, A. M., et al. (2007a), IONS (INTEX Ozonesonde Network Study, 2004). 1. Summertime UT/LS (Upper Troposphere/Lower Stratosphere) ozone over northeastern North America, *J. Geophys. Res.*, *112*, D12S12, doi: 10.1029/2006JD007441.

Thompson, A. M., et al. (2007b), Intercontinental Transport Experiment Ozonesonde Network Study (IONS, 2004): 2. Tropospheric Ozone Budgets and Variability over Northeastern North America, *J. Geophys. Res.*, *112*, D12S13, doi: 10.1029/2006JD007670.

Thompson, A. M., J. C. Witte, H. G. J. Smit, S. J. Oltmans, B. J. Johnson, V. W. J. H. Kirchhoff, F. J. Schmidlin (2007c), Southern Hemisphere Additional Ozonesondes (SHADOZ) 1998-2004 tropical ozone climatology. 3. Instrumentation, Station Variability, Evaluation with Simulated Flight Profiles, *J. Geophys. Res.*, 112, D03304, doi: 10.1029/ 2005JD007042.

Thompson, A. M., J. E. Yorks, S. K. Miller, J. C. Witte, K. M. Dougherty, G. A. Morris, D. Baumgardner, L. Ladino, and B. Rappenglueck (2008), Tropospheric ozone sources and wave activity over Mexico City and Houston during Milagro/Intercontinental Transport Experiment (INTEX-B) Ozonesonde Network Study, 2006 (IONS-06), *Atmos. Chem. Phys.*, **8**, 5113-5125.

Thompson, A.M., et al., (2009), Convective and wave signatures in ozone profiles over the equatorial Americas: Views from TC^4 (2007) and SHADOZ, *J. Geophys. Res.*, submitted, this issue.

Thompson, A.M., W.-K. Tao, K. E. Pickering, J. R. Scala, and J. Simpson (1997), Tropical deep convection and ozone formation, *Bull. Amer. Met. Soc., 78*, 1,043-1,054.

Toon, O. B., et al. (2009), Tropical Composition, Clouds, and Climate Coupling (TC4) Overview, *J. Geophys. Res.*, submitted, this issue.

Tuck, A.F. (1976), Production of nitrogen oxides by lightning discharges, *Quart. J. R. Met. Soc., 102*, 749 – 755.

Wenig, M. O., A. M. Cede, E. J. Bucsela, E. A. Celarier, K. F. Boersma, J. P. Veefkind, E. J. Brinksma, J. F. Gleason, and J. R. Herman, Validation of OMI tropospheric NO_2 column densities using direct-sun mode Brewer measurements at NASA Goddard Space Flight Center, *J. Geophys. Res.*, *113*, D16S45, doi:10.1029/2007JD008988, 2008.

Winterrath, T., T.P. Kurosu, A. Richter, and J.P. Burrows (1999), Enhanced O3 and NO2 in thunderstorm clouds: Convection or production, *Geophys. Res. Lett., 26*, 9, 1291 – 1294.

Wood, E.C., S.C. Herndon, T.B. Onasch, J.H. Kroll, M.R. Canagaratna, C.E. Kolb, D.R. Worsnop, J.A. Neuman, R. Seila, M. Zavala, and W.B. Knighton (2009), A case study of ozone production, nitrogen oxides, and the radical budget in Mexico City, *Atmos. Chem. Phys., 9(7)*, 2499 – 2516.

Zahn, A., C.A.M. Brenninkmeijer, P.J. Crutzen, D.D. Parrish, D. Sueper, G. Heinrich, H. Gusten, H. Fischer, M. Hermann, and J. Heintzenberg (2002), Electrical discharge source for tropospheric “ozone-rich transients,” *J. Geophys. Res., 107(D22)*, 4638, doi: 10.1029/2002JD002345.

Zavala, M., S.C. Herndon, E.C. Wood, J.T. Jayne, D.D. Nelson, A.M. Trimborn, E. Dunlea, W.B. Knighton, A. Mendoza, D.T. Allen, C.E. Kolb, M.J. Molina, and L.T. Molina (2009), Comparison of emissions from on-road sources using a mobile laboratory under various driving and operational sampling modes, *Atmos. Chem. Phys., 9(1)*, 1 – 14.

Zaveri, R.A., C.M. Berkowitz, L.I. Kleinman, S.R. Springston, P.V. Doskey, W.A., Lonneman, and C.W. Spicer (2003), Ozone production efficiency and NOx depletion in an urban plume: Interpretation of field observations and implications for evaluating O3-NOx-VOC sensitivity, *J. Geophys. Res., 108(D19)*, doi:10.1029/2002JD003144.

A.M. Bryan, Dept. of Amtospheric, Oceanic, and Space Sciences, University of Michigan, 2455 Hayword St., Ann Arbor, MI 48109-2143.

E.J. Bucsela, SRI International, 333 Ravenswood Ave., Menlo Park, CA 94025.

P.A. Kucera, Research Applications Laboratory, National Center for Atmospheric Research, 1850 Table Mesa Dr., Boulder, CO 80305.

D. Lutz and G.A. Morris, Dept. of Physics and Astronomy, Valparaiso University, Valparaiso, IN 46383. (gary.morris@valpo.edu).

K. Obenour and D. Slotke, Dept. of Meteorology, Valparaiso University, Valparaiso, IN 46383.

K.E. Pickering, Mail Code 613.3, NASA Goddard Space Flight Center, Greenbelt, MD 20771.

B.F. Taubman, Dept. of Chemistry, Appalachian State University, 525 Rivers St., Boone, NC 28608.

A.M. Thompson, Dept. of Meteorology, 510 Walker Building, Pennsylvania State University, University Park, PA 16802.

J.E. Yorks, Mail Code 613.1, NASA Goddard Space Flight Center, Greenbelt, MD 20771.

(Received ; revised ;
accepted .)

Paper number 2009JD007090.
zzzz-zzzz/xx/2000JD007090$xx.xx

Tables

Hours (UTC)	WWLLN Flashes	NPOL Flashes
0000 – 0800	9	0
0800 – 0900	4	0
0900 – 1000	36	9 (10)
1000 – 1100	61	0
1100 – 1200	34	44 (72)
1200 – 1300	174	240 (61)
1300 – 1400	160	450 (240)
1400 – 1500	92	670 (110)
1500 – 1600	6	600 (100)
1600 – 1700	0	240 (78)
1700 – 1800	1	11 (13)
1800 – 1900	2	1.7 (2.1)
1900 – 2000	9	4.3 (6.3)
2000 – 2400	150	108 (63)
Total 0900-1700	**563**	**2300 (300)**
TOTAL	**738**	**2400 (310)**

Table 1. Flashes detected by the World Wide Lightning Location Network and flashes calculated from cloud top heights estimated by the NPOL radar (uncertainties in parenthesis) near the Gulf of Panama on 5 August 2007. See text for details of each.

Trajectory Altitude (km)	Time from launch (s)	Balloon lat (deg)	Air mass lat (deg)	Balloon lon (deg)	Air mass lon (deg)	Separation (km)	Direction (deg)
	614	7.734	7.734	-80.269	-80.269	0.000	0
	2555	7.677	7.661	-80.337	-80.382	5.246	250
2.75 km	no data	no data	no data	no data	no data	no data	no data
	4629	7.660	7.597	-80.418	-80.492	10.816	230
	6208	7.654	7.550	-80.463	-80.551	15.103	220
	859	7.724	7.724	-80.277	-80.277	0.000	0
	2766	7.674	7.683	-80.346	-80.262	9.320	84
3.75 km	3459	7.671	7.657	-80.374	-80.260	12.672	97
	5010	7.654	7.605	-80.431	-80.261	19.494	106
	6535	7.655	7.565	-80.469	-80.235	27.614	111
	1134	7.722	7.722	-80.284	-80.284	0.000	0
	no data	no data	no data	no data	no data	no data	no data
4.75 km	3956	7.667	7.635	-80.393	-80.307	10.116	111
	5335	7.658	7.582	-80.440	-80.300	17.591	118
	6806	7.659	7.544	-80.476	-80.269	26.130	119

Table 2. Balloon trajectory and estimated air mass trajectories at three different altitudes within the 2.5 – 5.1 km layer in which the balloon oscillated. “No data” are reported when the balloon did not oscillate through the level of the air mass trajectory calculation. The “Direction” column indicates the compass heading from the balloon location to the estimated air mass location. Color coding matches that for the balloon data shown in Figures 12 – 15. See text for details.

Figure Captions

Figure 1. A comparison between the ozonesonde readings and NATIVE surface O_3 measurements at the time of launch. Agreement is good to within ~5% during the TC-4 campaign.

Figure 2. Low-level (0.7 elevation) PPI images of convection observed east of NPOL at 1311 UTC 05 Aug 2007. The color scale has units of radar reflectivity (dBZ).

Figure 3. Hourly mean surface O_3 data from 13 July – 9 August 2007 (black dots) and mean ± one standard deviation (dashed) recorded on NATIVE. The gray dots are the data from 5 August. During the period of the arrival of the convective cell (13 – 18 UTC), O_3 is decreased relative to the mean values.

Figure 4. Gridded ($1^0 \times 1^0$) OMI lightning NO_x in the Panama area on 5 August 2007. **(a)** Shows the larger region used for the first estimate, while **(b)** shows the smaller region in the Gulf of Panama used for the second estimate (see text).

Figure 5. The altitude vs. time of the ozonesonde flight on 5 August 2007 from Las Tablas, Panama shows the balloon oscillating 5 times between ~2.5 and ~5.0 km. The color coding of each ascent will be used in successive plots to identify changes with time of other measured parameters.

Figure 6. Ozone vs. altitude on the ascents as the balloon oscillated on the 5 August 2007 flight, with color coding to match the ascents identified in Fig. 3.5.1.

Figure 7. Wind speed (thick) and direction (thin) as determined from the ozonesonde GPS data. The balloon moved through a region of vertical shear, resulting in the separation of the balloon trajectory from the trajectories of the air masses the sonde sampled. See text and Table 2 for further details.

Figure 8. Calculated dO_3/dt vs. altitude for the ascents of the flight on the 5 August 2007 flight, with color coding to match the ascents identified in Fig. 3.5.1. See text for details.

Figure 9. The change in potential temperature from the first to the last ascent vs. altitude for the flight of 5 August 2007.

Figure 10. Ozone vs. potential temperature for the first and last ascents of the flight of 5 August 2007 shows that the changes cannot be due to descent of the air mass alone.

MORRIS ET AL.: OZONE PRODUCTION IN A CONVECTIVE CELL

Figure 1

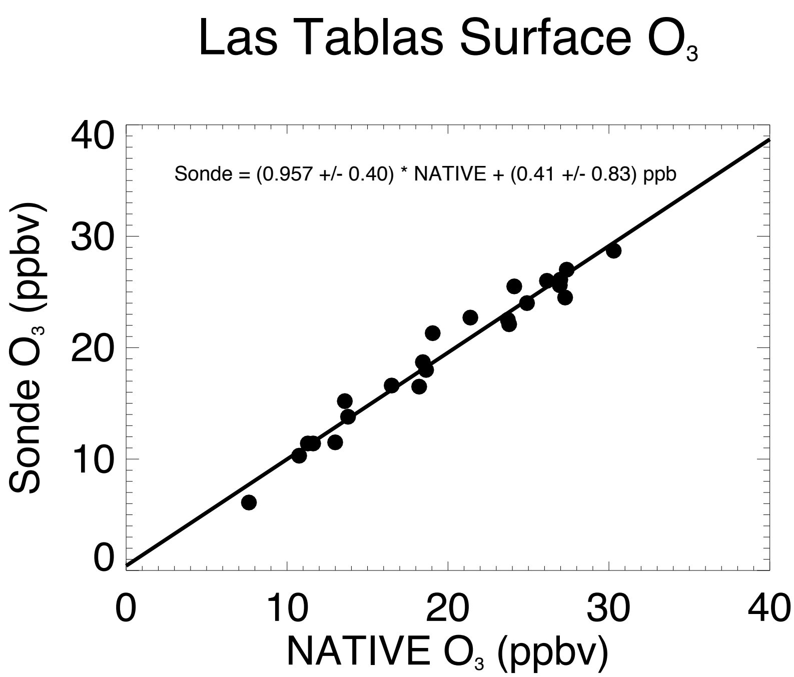
Las Tablas Surface O3
Sonde = (0.957 +/- 0.40) * NATIVE + (0.41 +/- 0.83) ppb
40
30
20
10
0
0
10
20
30
40
Sonde O3 (ppbv)
NATIVE O3 (ppbv)

Figure 2

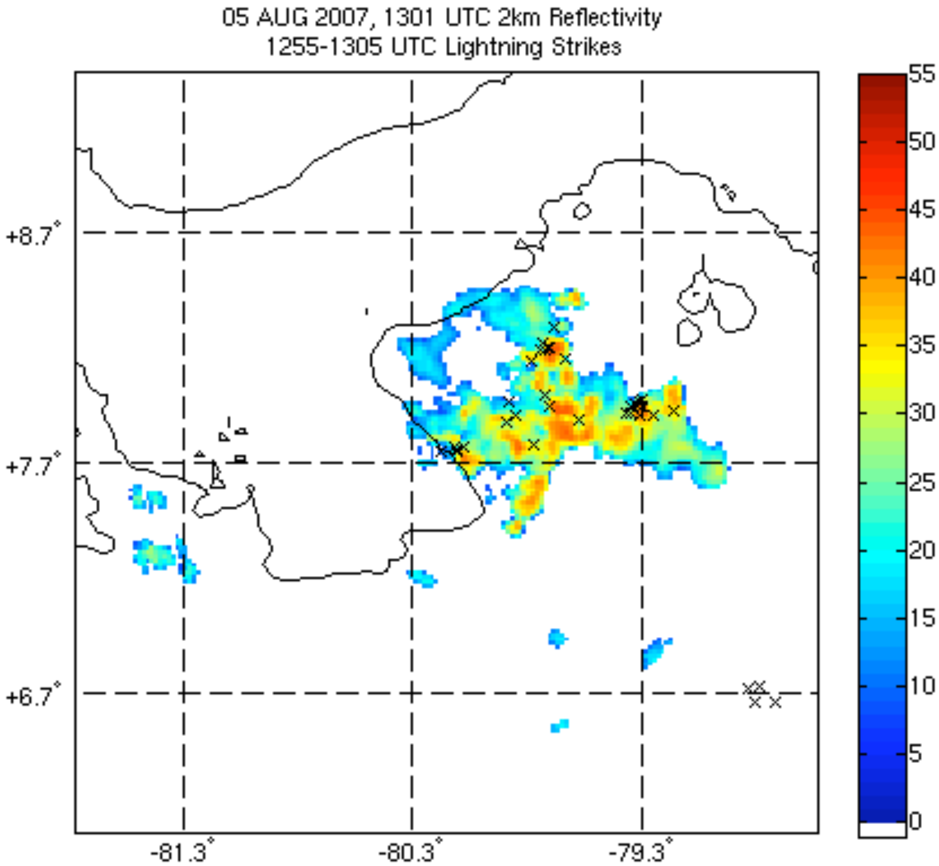
05 AUG 2007, 1301 UTC 2km Reflectivity
1255-1305 UTC Lightning Strikes
+8.7°
+7.7°
+6.7°
-81.3°
-80.3°
-79.3°
55
50
45
40
35
30
25
20
15
10
5
0

Figure 3

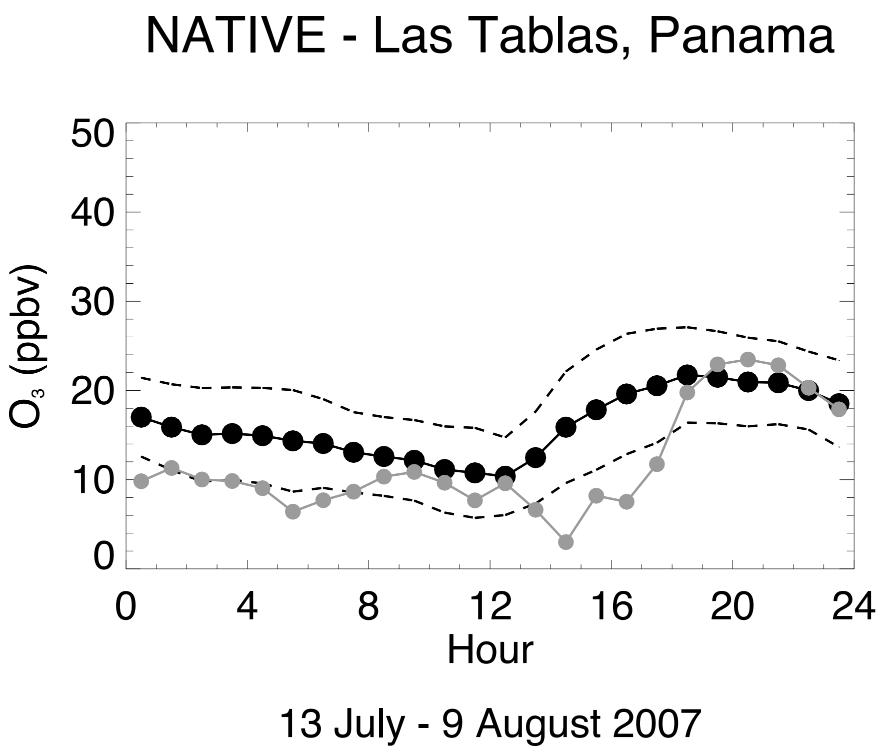
NATIVE - Las Tablas, Panama
50
40
30
20
10
0
O3 (ppbv)
0
4
8
12
16
20
24
Hour
13 July - 9 August 2007

Figure 4

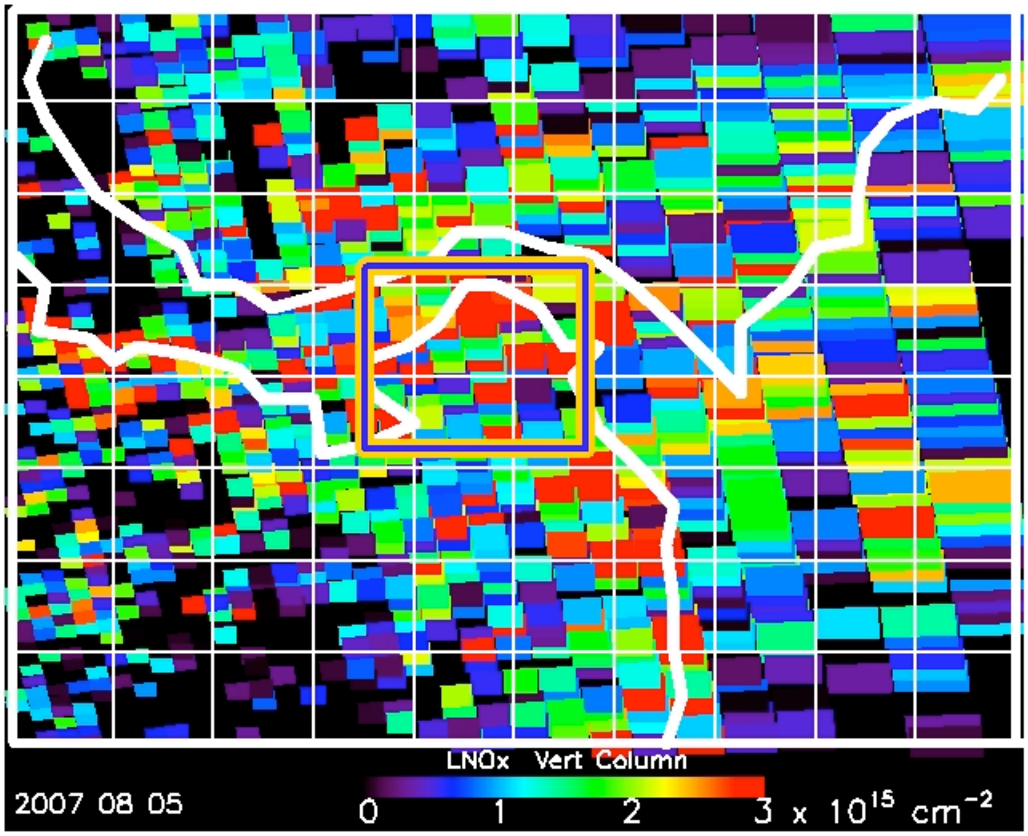

Figure 5

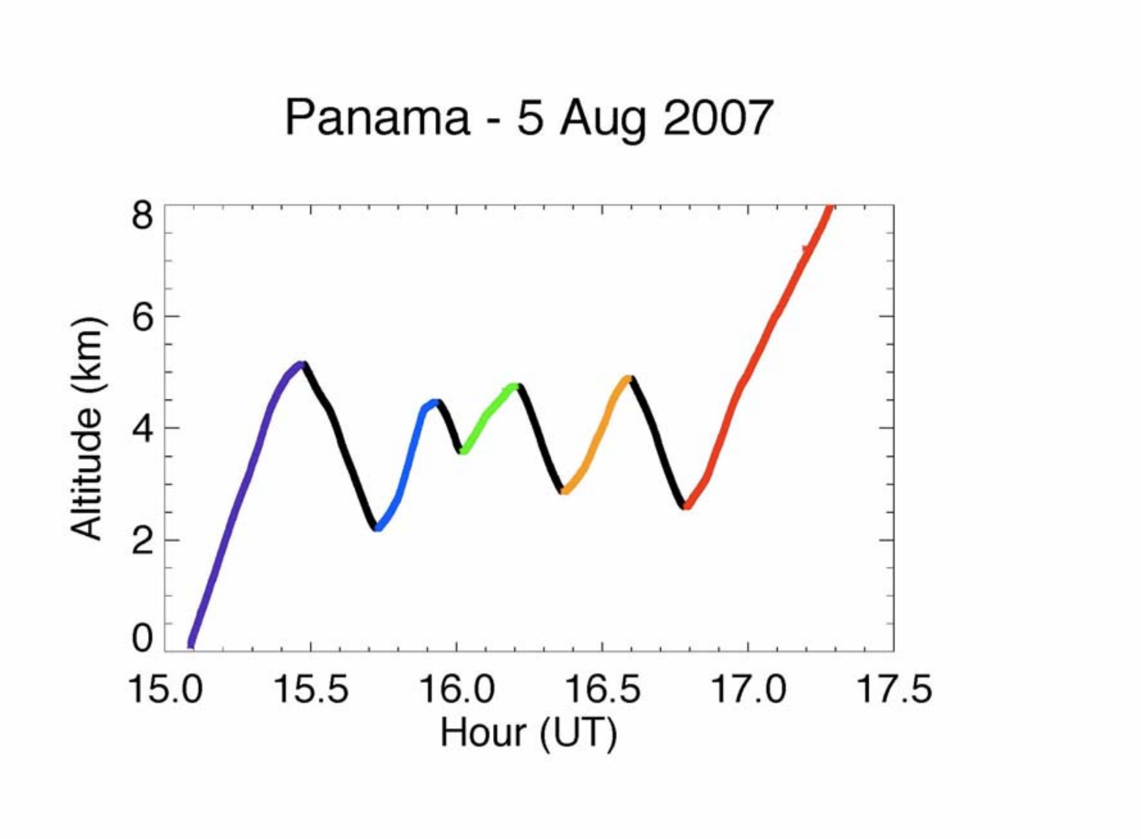
Panama - 5 Aug 2007
8
6
4
2
0
Altitude (km)
15.0
15.5
16.0
16.5
17.0
17.5
Hour (UT)

Figure 6

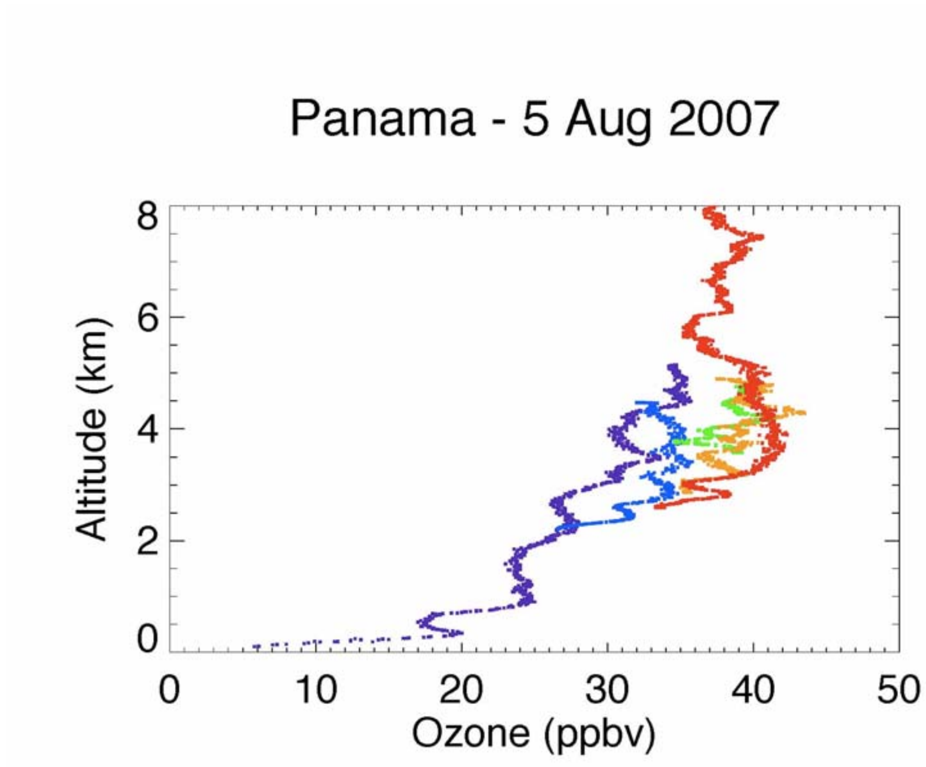

Figure 7

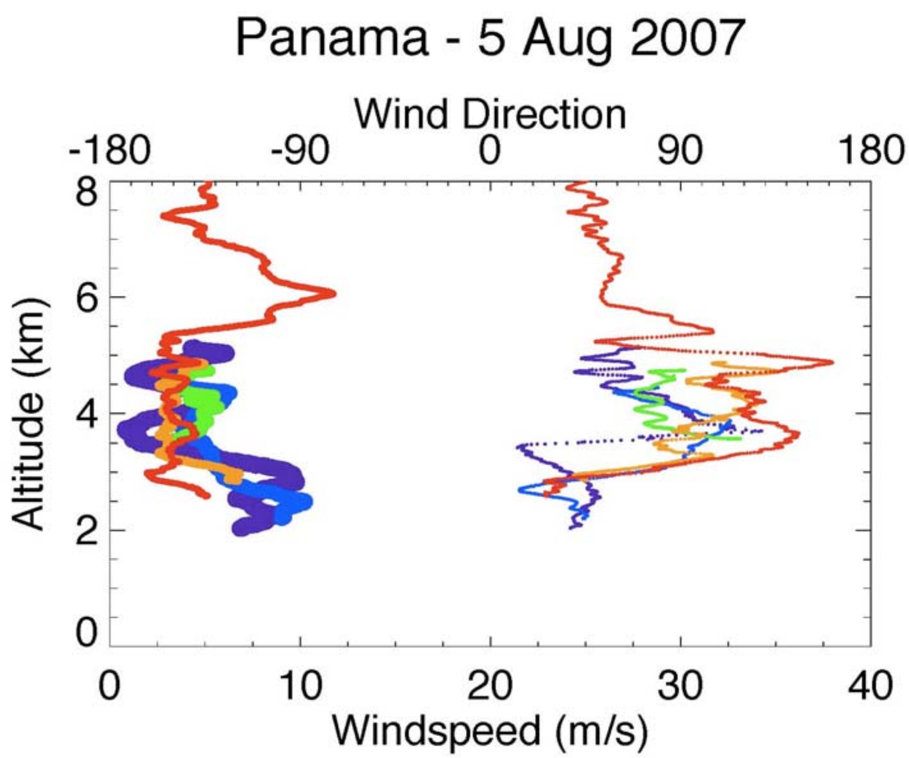
Panama - 5 Aug 2007
Wind Direction
-180
-90
0
90
180
8
6
4
2
0
Altitude (km)
0
10
20
30
40
Windspeed (m/s)

884
885 # Figure 8

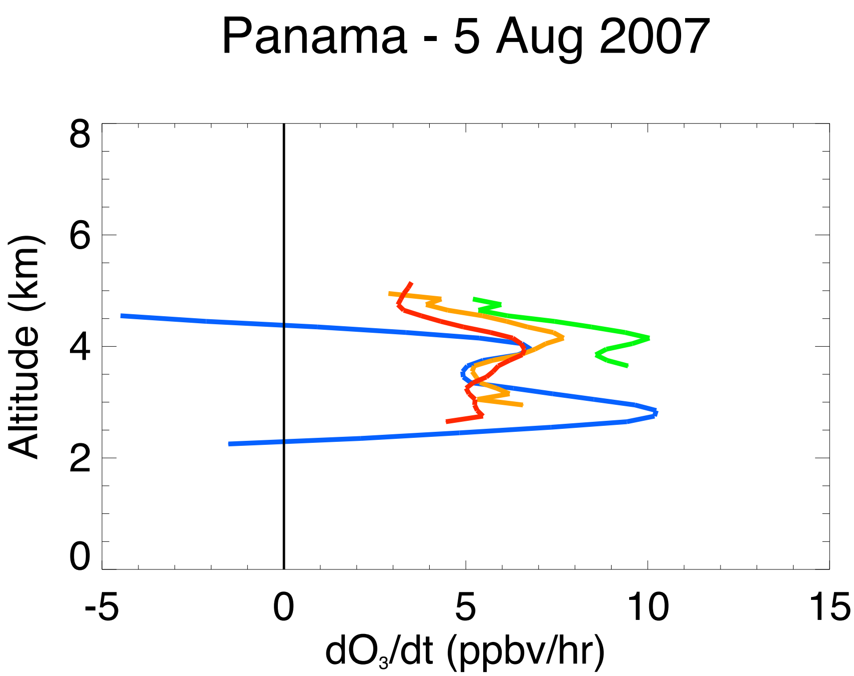

886

Figure 9

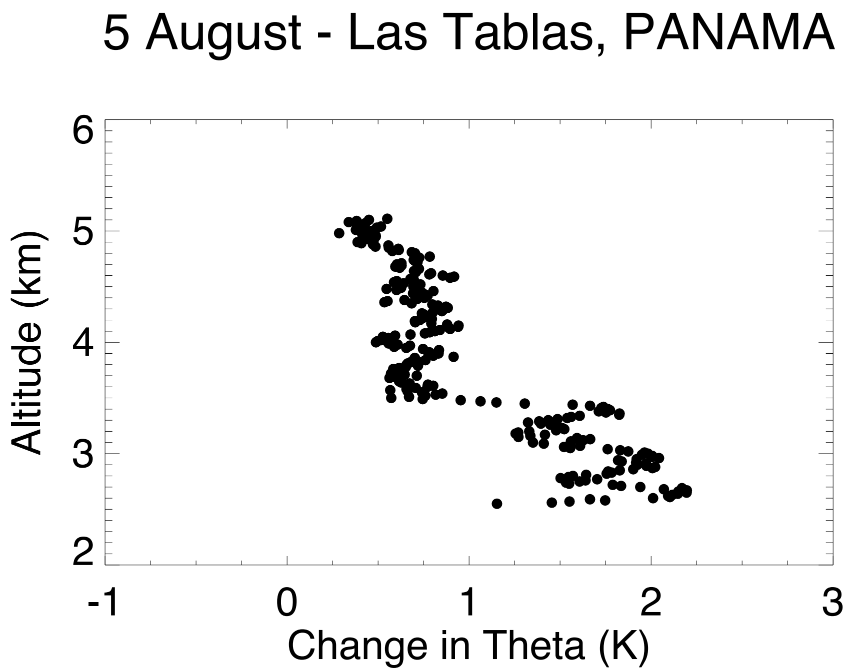
5 August - Las Tablas, PANAMA
Altitude (km)
6
5
4
3
2
-1
0
1
2
3
Change in Theta (K)

Figure 10

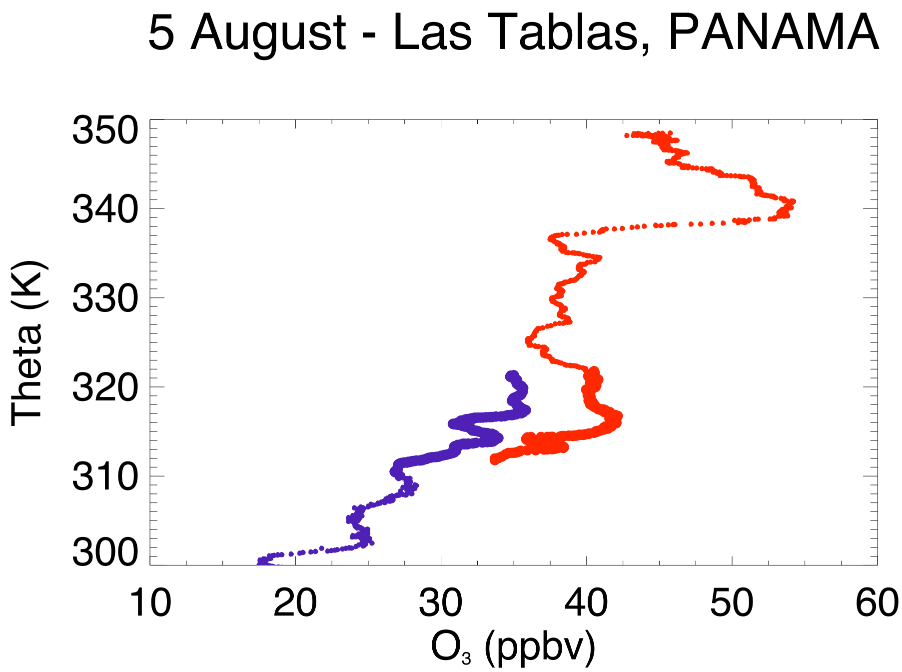
5 August - Las Tablas, PANAMA
Theta (K)
350
340
330
320
310
300
10
20
30
40
50
60
O3 (ppbv)